Molecular Microbiology (2013) 87(3), 553–568 ■
doi:10.1111/mmi.12115
First published online 11 December 2012

DnaN clamp zones provide a platform for spatiotemporal coupling of mismatch detection to DNA replication

Justin S. Lenhart,[1] Anushi Sharma,[2] Manju M. Hingorani[2] and Lyle A. Simmons[1]*
[1]*Molecular, Cellular, and Developmental Biology, University of Michigan. Ann Arbor, MI, USA.*
[2]*Department of Molecular Biology and Biochemistry, Wesleyan University. Middletown, CT, USA.*

Summary

Mismatch repair (MMR) increases the fidelity of DNA replication by identifying and correcting replication errors. Processivity clamps are vital components of DNA replication and MMR, yet the mechanism and extent to which they participate in MMR remains unclear. We investigated the role of the *Bacillus subtilis* processivity clamp DnaN, and found that it serves as a platform for mismatch detection and coupling of repair to DNA replication. By visualizing functional MutS fluorescent fusions *in vivo*, we find that MutS forms foci independent of mismatch detection at sites of replication (i.e. the replisome). These MutS foci are directed to the replisome by DnaN clamp zones that aid mismatch detection by targeting the search to nascent DNA. Following mismatch detection, MutS disengages from the replisome, facilitating repair. We tested the functional importance of DnaN-mediated mismatch detection for MMR, and found that it accounts for 90% of repair. This high dependence on DnaN can be bypassed by increasing MutS concentration within the cell, indicating a secondary mode of detection *in vivo* whereby MutS directly finds mismatches without associating with the replisome. Overall, our results provide new insight into the mechanism by which DnaN couples mismatch recognition to DNA replication in living cells.

Introduction

Mismatch repair (MMR) increases the fidelity of DNA replication by identifying and correcting errors made by the replicative DNA polymerase (for review: Schofield and Hsieh, 2003; Kunkel and Erie, 2005). Upon detection of an error, MMR orchestrates its removal and accurate resynthesis of the surrounding DNA, ultimately increasing the fidelity of DNA replication by several hundred-fold (for review: Schofield and Hsieh, 2003; Kunkel and Erie, 2005; Iyer *et al.*, 2006). Due to this important role in maintaining genome stability, MMR is found in all domains of life, with a high degree of conservation specifically among MutS and MutL proteins (Culligan *et al.*, 2000). In bacteria, deletion of either *mutS* or *mutL* homologues leads to an increased mutation rate (Cox *et al.*, 1972; Prudhomme *et al.*, 1989; Ginetti *et al.*, 1996; Davies *et al.*, 2011; Cooper *et al.*, 2012). This mutator phenotype is known to accelerate acquisition of multidrug-resistant strains in hospital settings, while also enabling increased survival of bacterial pathogens in harsh environments, including growth inside the lungs of cystic fibrosis patients (Oliver *et al.*, 2000; Denamur *et al.*, 2002; Prunier *et al.*, 2003; Roman *et al.*, 2004; Watson *et al.*, 2004; Mena *et al.*, 2008; Turrientes *et al.*, 2010; and for review: Chopra *et al.*, 2003; Oliver and Mena, 2010). MMR defects in eukaryotes are characterized by hypermutability and microsatellite instability; both of which have been linked to an increased predisposition for spontaneous tumorigenesis, as well as inherited conditions such as Lynch syndrome and Turcot syndrome (Fishel *et al.*, 1993; Hamilton *et al.*, 1995; Nystrom-Lahti *et al.*, 2002; Peltomaki, 2005).

In bacteria, the MutS homodimer initiates MMR by detecting base–base mismatches or small insertion/deletion loops (IDLs) (Su and Modrich, 1986). In eukaryotes, base–base mismatches and small IDLs (one or two extrahelical nucleotides) in DNA are primarily recognized by Msh2–Msh6 (MutSα), while larger IDLs (1–15 extrahelical nucleotides) are recognized by Msh2–Msh3 (MutSβ) heterodimers (Prolla *et al.*, 1994; Alani *et al.*, 1995; Habraken *et al.*, 1996; Palombo *et al.*, 1996). In all systems, following mismatch or IDL detection by a MutS homologue, MutL (MutLα or MutLβ in eukaryotes) is recruited to the site of the mismatch in a reaction that requires ATP (Schofield *et al.*, 2001b). Following this step, MutL is hypothesized to facilitate removal of the mismatch by co-ordinating numerous DNA transactions including endonuclease nicking, helicase-driven unwinding and excision of the segment containing the misincorporated base(s) (Lahue *et al.*, 1989).

Accepted 21 November, 2012. *For correspondence. E-mail lasimm@umich.edu; Tel. (+1) 734 647 2016; Fax (+1) 734 647 0884.

Since replicative DNA polymerases have high fidelity, base pairing errors occur at a low frequency of one in 10^6–10^7 correctly paired bases (Schaaper, 1993, and for review: Kunkel, 1992; Kunkel and Bebenek, 2000). In addition to the challenges posed by the low rate of error formation, base mispairs may also be obscured by DNA supercoiling, compaction and protein binding. MutS must also contend with other active processes on the DNA, including transcription, when searching for mismatches and IDLs in DNA (for review on chromosome organization: Jackson *et al.*, 2012). Given these challenges, it has been proposed that MutS is coupled to DNA replication forks in order to facilitate efficient mismatch detection where mismatches are newly formed, and where the DNA is more likely to be free of protein impediments (Smith *et al.*, 2001; Simmons *et al.*, 2008). In support of this model, cytological studies conducted in *Bacillus subtilis, Saccharomyces cerevisiae* and human cells have shown that prokaryotic MutS–GFP and eukaryotic MutSα (Msh6–mCherry) form foci that are often coincident with DNA replication foci *in vivo* (Kleczkowska *et al.*, 2001; Smith *et al.*, 2001; Simmons *et al.*, 2008; Hombauer *et al.*, 2011a). Furthermore, in *B. subtilis*, MutS and mismatches were shown to alter localization of an essential DNA polymerase (Klocko *et al.*, 2011). These results suggest that MutS is spatially co-ordinated with active replisomes in *B. subtilis*, *S. cerevisiae* and human cells. In addition to possible spatial coupling between MMR and DNA replication, *S. cerevisiae* MMR was shown to be defective when Msh6 was unavailable during S phase (DNA replication), supporting the importance of temporal coupling of MutSα to DNA replication in eukaryotes (Hombauer *et al.*, 2011b).

Studies in various model organisms indicate that DNA replication processivity clamps function in MMR (Flores-Rozas *et al.*, 2000; Kleczkowska *et al.*, 2001; Lee and Alani, 2006; Lopez de Saro *et al.*, 2006; Shell *et al.*, 2007; Simmons *et al.*, 2008; Hombauer *et al.*, 2011a). Processivity clamps exist as either a homodimer in bacteria (DnaN) or a homotrimer in archaea and eukaryotes (PCNA) (Kong *et al.*, 1992; Krishna *et al.*, 1994; Matsumiya *et al.*, 2001). These clamps are loaded onto the 3′ termini of DNA by the clamp loader complex (e.g. Jeruzalmi *et al.*, 2001; Bowman *et al.*, 2004; Georgescu *et al.*, 2008), and once loaded, DnaN and PCNA confer processive activity to replicative polymerases by tethering the polymerase to the DNA template (Huang *et al.*, 1981; Stukenberg *et al.*, 1991). MutS homologues contain a conserved DnaN clamp-binding motif, or PIP box (PCNA Interacting Protein) in eukaryotes, that mediates interactions between MutS proteins and their cognate processivity clamps (Flores-Rozas *et al.*, 2000; Kleczkowska *et al.*, 2001; Lee and Alani, 2006; Lopez de Saro *et al.*, 2006; Shell *et al.*, 2007; Simmons *et al.*, 2008; Hombauer *et al.*, 2011a; Monti *et al.*, 2012). Studies in *B. subtilis* showed that deletion of the unstructured region of MutS (MutS800) containing a putative DnaN clamp-binding motif, reduced interaction with DnaN, yet MutS800 maintained the ability to preferentially bind mismatched DNA *in vitro* (Simmons *et al.*, 2008). *In vivo*, the *mutS800* allele eliminated functional MMR, and when translationally fused to *gfp*, failed to form foci demonstrating that although proficient in mismatch detection, MutS800 was defective for forming repair complexes *in vivo* (Simmons *et al.*, 2008). Recent work in *S. cerevisiae* demonstrates that PCNA-associated MutSα accounts for 10–15% of MMR *in vivo*, and that Msh6–GFP (MutSα) foci are dependent upon interaction with PCNA through the Msh6 PIP box (Hombauer *et al.*, 2011a). Processivity clamps are also proposed to function in downstream steps of MMR, such as facilitating activation of endonuclease activity in MutL homologues (Kadyrov *et al.*, 2006; Pillon *et al.*, 2010; 2011; Pluciennik *et al.*, 2010) and in re-synthesis of the gap in DNA following strand excision (Gu *et al.*, 1998; Umar *et al.*, 1996; for review: Larrea *et al.*, 2010; Lenhart *et al.*, 2012). While it is clear that interactions between MutS and processivity clamps play a role in MMR (e.g. Umar *et al.*, 1996; Gu *et al.*, 1998), important questions remain about their significance (Clark *et al.*, 2000; Flores-Rozas *et al.*, 2000; Lopez de Saro *et al.*, 2006), the mechanism(s) by which clamps influence MMR *in vivo* and the step during MMR that require processivity clamp interaction. Three main models have been used to explain the role of processivity clamps in MMR. These models include the hypothesis that clamps directly aid in mismatch binding (Flores-Rozas *et al.*, 2000; Lau and Kolodner, 2003; Simmons *et al.*, 2008), clamps recruit MutS to sites of DNA replication (Kleczkowska *et al.*, 2001; Hombauer *et al.*, 2011a) or that clamps are required for DNA synthesis after mismatch removal and do not have an earlier role during MMR (Pluciennik *et al.*, 2009). Other key questions are, what step of repair is affected by the clamp, as well as how MutS dynamics on DNA are effected by the presence of the clamp as MutS searches for and initiates repair of rare mismatches formed during replication.

In vivo studies of DNA replication in *B. subtilis* show that the DnaN processivity clamp exists in a ‘clamp zone’ immediately following the progressing replication forks. DnaN clamps are retained on nascent DNA during Okazaki fragment maturation and accumulate until a steady-state level is reached between actively loaded and unloaded clamps (Su’etsugu and Errington, 2011). Because DnaN clamp zones trail the replication fork, these zones have the potential to serve as platforms that maintain the spatial and temporal relationship between mismatch recognition and active replication forks. In this work, we used several separation-of-function MutS mutants that are defective in either mismatch detection or DnaN binding to determine when and where during repair the MutS–DnaN interaction

is mechanistically significant in live cells. Using functional *mutS–gfp* fusions expressed from the *mutS* native locus, we report that DnaN clamp zones position MutS at newly replicated DNA prior to, and independent of, mismatch binding. After mismatch detection, MutS no longer remains coincident with the replication machinery, instead localizing to sites of repair. Importantly, ~ 90% of MMR *in vivo* is initiated through DnaN clamp zones, revealing a heavy reliance by MutS on the clamp during the initial steps of repair. We used the MutS800 mutant to uncouple MMR from DnaN and found that this mutant could account for only ~ 10% of *in vivo* repair. Remarkably, we were able to restore DnaN-independent MMR to wild-type levels by increasing the cellular levels of MutS800, illustrating that the functional significance of the DnaN–MutS interaction lies in maximizing the efficiency of mismatch detection *in vivo*. Interestingly, mismatch detection appeared to occur on replication fork proximal DNA. This observation contrasts with models where MMR is initiated through detection of a mismatch distal to the replisome and nascent DNA. Our findings indicate that *B. subtilis* MutS relies on mismatch detection on nascent DNA for efficient repair. Ultimately, by having MutS bind to DnaN clamp zones that closely trail replication forks, MMR and DNA replication become tightly coupled, allowing for efficient mismatch detection, MutL activation and subsequent repair in *B. subtilis* cells.

Results

B. subtilis *MutSF30A is MMR deficient due to loss of mismatch binding specificity*

In order to determine if mismatch binding is necessary for MutS localization, we monitored MutSF30A, which has a mutation that should abolish mismatch recognition (Malkov *et al*., 1997). During high-affinity interaction between MutS and mismatched DNA, the phenylalanine residue in the conserved GXFY$(X)_5$DA motif stacks with the mismatched or unpaired base (Fig. 1A) (Lamers *et al*., 2000; Obmolova *et al*., 2000). Substitution of phenylalanine to alanine eliminates mismatch detection *in vitro* and functional MMR *in vivo* in several organisms (Malkov *et al*., 1997; Bowers *et al*., 2000; Schofield *et al*., 2001a). This mutation does not disrupt the ATPase mechanism, indicating that MutSF30A activities other than mismatch binding are unaffected (Jacobs-Palmer and Hingorani, 2007).

We tested the corresponding *mutSF30A* mutation for the ability to support both mismatch binding *in vitro* and functional repair in *B. subtilis*. We purified *B. subtilis* MutSF30A using standard chromatography techniques without the use of an affinity tag (Fig. 1B). We found that purified MutS binds a T-bulge DNA substrate (containing an extrahelical thymidine) selectively with a K_d of 24 nM, while MutSF30A shows little binding to either a T-bulge or a homoduplex DNA substrate, precluding us from calculating a K_d (Fig. 1C). Furthermore, we verified that the F30A mutation did not have an adverse affect on MutS binding to DnaN. An immunodot blot analysis shows comparable retention of DnaN by MutS and MutSF30A (Fig. 1D).

MutSF30A function was also tested *in vivo* by introducing an unmarked *mutSF30A* allele at the native *mutS* locus by allelic replacement (see *Experimental procedures*). Immunoblot analysis confirmed that the mutant MutS protein, as well as the downstream gene product MutL, accumulated to wild-type levels *in vivo* (Fig. 1E). Using spontaneous rifampicin resistance as an indicator for mutation rate, we found that the *mutSF30A* allele conferred a mutation rate of 155.4×10^{-9} mutations per generation, significantly higher than the mutation rate of the wild-type strain, which was 1.82×10^{-9} mutations per generation (Table 1). The *mutSF30A* mutation rate was indistinguishable from a strain with the *mutSL::spec* allele, which eliminates all *in vivo* MMR, showing an ~ 85-fold increase in mutagenesis to 154.5×10^{-9} mutations per generation. With these data we conclude that the *B. subtilis mutSF30A* allele is MMR defective *in vivo* due to a loss in mismatch binding specificity.

MutSF30A–GFP forms foci on DNA independent of mismatch binding

After demonstrating that *B. subtilis* MutSF30A is defective for mismatch binding, we sought to determine whether mismatch binding is a prerequisite for localization of MutS into discrete foci *in vivo*. We first determined that the *mutS–gfp* native locus allele exhibits ~ 90% of wild-type MMR activity, indicating that the *gfp* fusion has little impact on MutS function *in vivo* (Table S1). MutS–GFP foci were detected in only ~ 9% of untreated, exponentially growing cells, whereas treatment with the mismatch forming agent 2-aminopurine (2-AP) resulted in > 45% of cells with MutS–GFP foci (Figs 2A and C and S1). A similar increase in MutS–GFP foci occurred following introduction of a DNA polymerase mutant, *polC mut-1* defective in proofreading (herein referred to as $polC^{exo-}$), which substantially increases the frequency of errors during DNA replication (Sanjanwala and Ganesan, 1991). MutS–GFP focus formation was observed in ~ 25% of cells when $polC^{exo-}$ was the sole source of the replicative DNA polymerase in the cell (Fig. 2C). These results demonstrate that MutS–GFP focus formation responds to natural mismatches formed by normal bases during DNA replication.

To test if mismatch binding was a prerequisite for MutS localization, we built a *mutSF30A–gfp* reporter allele at its native locus. Strikingly, MutSF30A–GFP formed foci during exponential growth in ~ 6% of cells (Fig. 2A and C). As a control, we determined via immunoblot that the

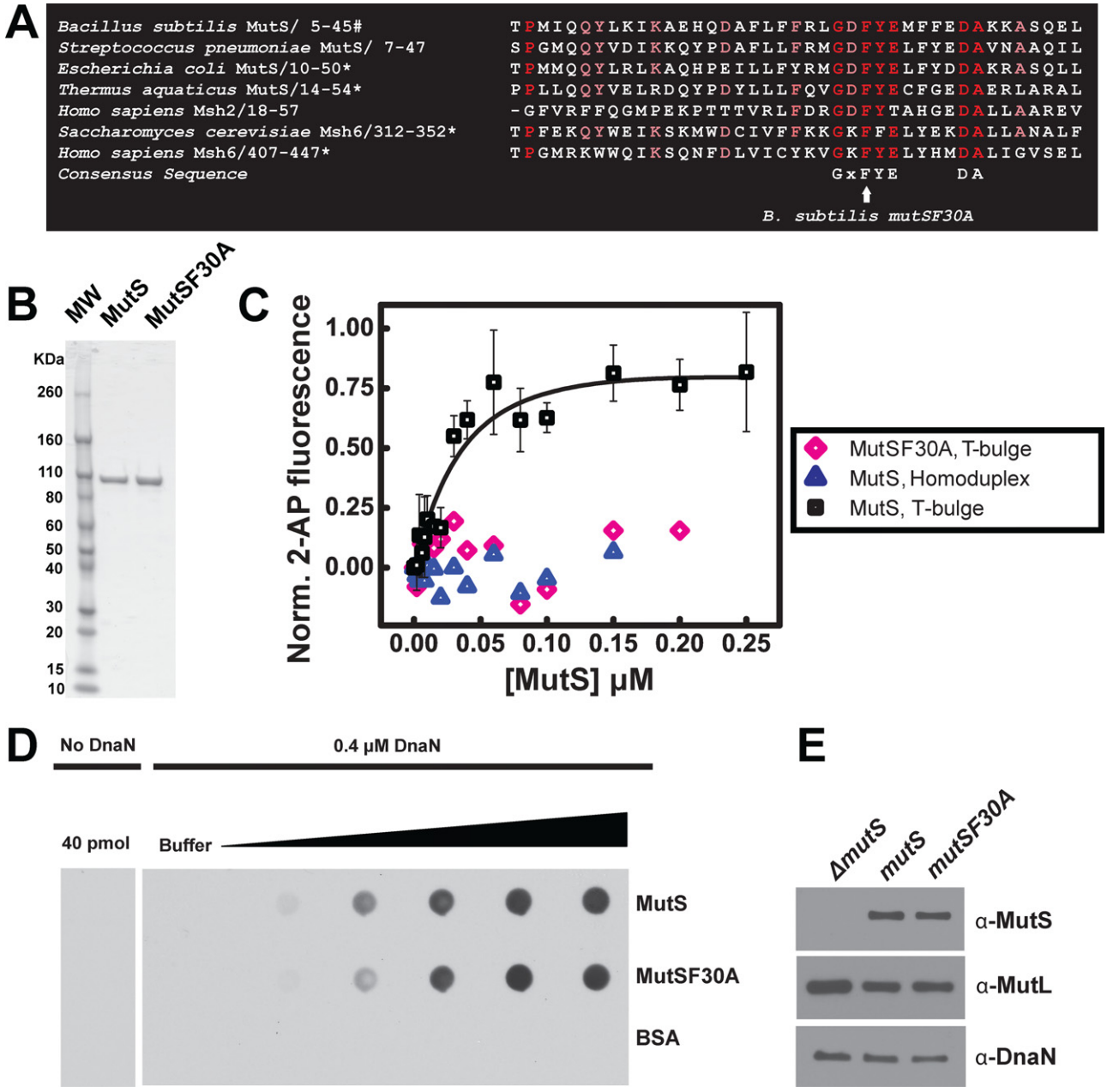

Fig. 1. MutSF30A is unable to bind mismatches *in vitro*.
A. The following conserved motif necessary for mismatch binding (GXFYXXXXXDA) is found in a wide range of eukaryotic and prokaryotic MutS homologues. (*) Substitution of the conserved phenylalanine residue (F) eliminates mismatch binding *in vitro* and prevents MMR *in vivo*.
B. One microgram of purified MutS and MutSF30A protein electrophoresed on a 4–15% SDS-PAGE gradient gel.
C. *In vitro* binding of MutS and MutSF30A to T-bulge substrate. Legend: black squares and pink diamonds show MutS and MutSF30A interaction with T-bulge containing DNA, respectively, and blue triangles show MutS interaction with homoduplex DNA.
D. An immunodot blot (far Western) analysis was performed to monitor interaction between MutS or MutSF30A with DnaN. Purified MutS and MutSF30A were blotted onto a nitrocellulose membrane over a range of 0.625 pmol to 40 pmol of dimer. Purified DnaN was incubated with the membrane and probed with affinity-purified antisera against DnaN in a 1:500 dilution. Shown (left most blot) is the purified antisera control against purified MutS and MutSF30A. Shown (right most blot) is the retention of DnaN by MutS and MutSF30A as described in *Experimental procedures*.
E. *In vivo* steady-state levels of MutS, MutL and DnaN. A total of 5 μg of cell extract derived from the indicated strain was electrophoresed and immunoblotted in the indicated lanes.

Table 1. *mutSF30A* is defective for mismatch repair (MMR) *in vivo*.

Relevant genotype	No. of cultures	Mutation rate (10^{-9} mutations per generation) ± [95% CI]	Relative mutation rate	Total MMR activity (%)
PY79 (wild type)	51	1.82 [1.14–2.37]	1	100
mutSL::spc	23	154.4 [146.6–162.2]	84.9	0
mutSF30A	24	155.9 [147.5–163.3]	85.5	–0.7
dnaN5	30	39.2 [33.7–44.7]	21.6	75.5

Mismatch repair proficiency and analysis of the mutation rate of the *mutSF30A* strain compared with wild-type cells and MMR-deficient cells. The bracketed values represent the lower and upper bounds of the 95% confidence limit.

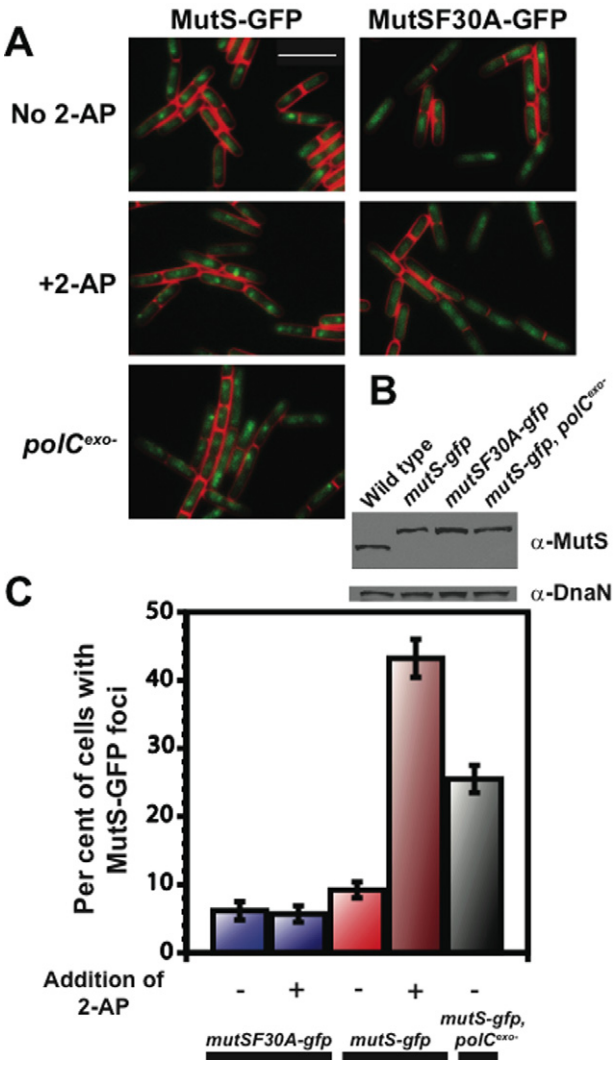

Fig. 2. MutS–GFP forms foci independent of mismatch formation.
A. Representative images of MutS–GFP or MutSF30A–GFP foci in cells with or without 600 μg ml^{-1} 2-AP. The white bar is 4 μm.
B. An immunoblot of the indicated MutS derivative and DnaN as a loading control.
C. Bar graph of the groups represented in (A) showing the percentage of cells with MutS–GFP foci. Total number of cells scored for each condition was from left to right: $n = 1234$, 1410, 2380, 1222 and 1797.

cellular level of MutS and MutSF30A–GFP were indistinguishable (Fig. 2B). When MutSF30A–GFP cells were challenged with 2-AP, we did not observe an increase in foci above ~ 6% (Fig. 2C) supporting our data that MutSF30A is defective in mismatch recognition. Furthermore, MutL–GFP focus formation in *mutSF30A* cells was not stimulated by 2-AP treatment, indicating that MutS must be able to bind a mismatch in order to efficiently activate the downstream steps of repair *in vivo*, including recruitment of MutL (Supporting results and Fig. S2). Thus, MutSF30A fails to detect and respond to 2-AP formed mismatches *in vivo*, consistent with the above data showing loss of mismatch binding *in vitro* (Fig. 1C).

Interestingly, we did observe a small, though statistically significant difference in the per cent of cells with foci between untreated *mutSF30A–gfp* and *mutS–gfp* cells (Figs 2C and S1). This result is not explained by differences in binding of MutS or MutSF30A to DnaN since both proteins bind DnaN equally. Because we expect a small subset of cells to undergo MMR in the functional *mutS–gfp* background, we suggest that the slightly greater percentage of cells with MutS–GFP foci relative to the MutSF30A–GFP in untreated cells represents MutS–GFP foci engaged in repair. We conclude that MutS forms two types of foci: one licensed by mismatch detection and one that is mismatch-detection independent. Together our results demonstrate that MutS forms foci on DNA independent of, or prior to, mismatch binding in live cells.

MutS is staged at active replisomes prior to mismatch recognition

We investigated the localization dynamics of MutS foci before and after mismatch detection in order to better understand the spatial-temporal coupling of MutS to the replisome. We define the replisome as replication-associated proteins (replicative polymerases, clamp loader components, processivity clamp, etc.) that localize as discrete foci at replication forks *in vivo*. In *B. subtilis*, the replisome occupies characteristic subcellular positions denoting the site of DNA synthesis (Lemon and Grossman,

1998; Migocki *et al*., 2004; Berkmen and Grossman, 2006). Immediately after replication initiation from *oriC*, origin regions and replicated DNA translocate away from the replisome towards the opposite cell poles (Webb *et al*., 1997; Teleman *et al*., 1998). Previously, it was shown that *B. subtilis* MutS–YFP colocalizes with the replisome in ~ 48% of cells (Smith *et al*., 2001). As shown above, the percentage of cells with MutS–GFP foci increase following 2-AP treatment (Fig. 2) (Smith *et al*., 2001; Simmons *et al*., 2008; Klocko *et al*., 2011), indicating that more repair complexes are formed. As DNA replication progresses, the newly replicated chromosomal DNA moves towards the cell poles (Webb *et al*., 1997), presumably taking replication errors away from the replisome. Thus, we hypothesized that the MutS–GFP foci would initially associate with mismatches in DNA at or near the replisome, and as repair and replication continued, the mismatch•MutS complex would move towards the cell poles, reducing colocalization with the replisome.

Initially, we tested our ability to spatially resolve replicated DNA from the replisome by monitoring the colocalization of CFP–Spo0J with DnaX–YFP. We grew cells slowly so that most cells would have one or two replisome foci during this analysis (Fig. S3) (see *Experimental procedures*). Spo0J, which localizes to and helps organize the origin of replication (*oriC*), should only colocalize with the clamp loader protein DnaX during replication of the origin region, and then translocate away from the replisome to the cell pole (Gruber and Errington, 2009; Sullivan *et al*., 2009). We found that in cells containing a single DnaX–mYFP focus, only 12.8% of replisome foci colocalized with CFP–Spo0J ($n = 297$). Furthermore, inspection of these cells shows that most single replisome cells contain the expected origin–replisome–origin localization pattern along their longitudinal axis (Fig. 3).

To test our hypothesis that MutS moves away from the replisome after mismatch binding, we introduced functional *dnaX–gfp* and *mutS–gfp* alleles (> 90% MMR activity) (Table S1) into *B. subtilis* cells, with both fusions placed at their native locus and under control of their native promoters. During exponential growth, MutS–YFP foci colocalized with the replisome in ~ 56% of cells containing at least one DnaX–CFP focus and one MutS–YFP focus (Fig. 3B). When cells were treated with 2-AP to form mismatches, we observed a significant decrease in colocalization to ~ 35% ($P = 2.03 \times 10^{-5}$) (Fig. 3B and D). These data support the hypothesis that mismatch recognition by MutS–YFP reduces colocalization with the replisome.

When the same experiment was performed with *mutSF30A–gfp*, we observed that MutSF30A–YFP foci colocalized with the replisome ~ 73% of the time in the absence of 2-AP challenge (Fig. 3C and D). When this strain was treated with 2-AP, there was no significant statistical difference in the position of MutSF30A–YFP foci compared with the untreated group (~ 70.1% colocalized: $P = 0.277$). Thus, lacking the ability to detect mismatches in DNA, MutSF30A–YFP remains colocalized with the replisome. These results lead us to conclude that MutS–GFP foci, when not bound to mismatches, are staged near the active replisome, possibly due to physical coupling with a replication protein. Subsequently, upon encountering a mismatch, MutS disengages from the advancing replisome and remains behind on nascent DNA to direct the remaining steps in repair. This result provides insight into how mismatch recognition affects the dynamic association of MutS with the replisome *in vivo*.

Based on this model, we hypothesized that if MutS is positioned on newly replicated DNA through interaction with a replisome protein, then increasing expression of MutS or MutSF30A should increase the number of mismatch-independent foci by promoting this interaction *in vivo*. To this end, we constructed an in frame *mutS* deletion that maintains transcriptional control of *mutL* from its native promoter (Figs 1D and S4). We then expressed MutS–GFP or MutSF30A–GFP from an ectopic locus driven by an IPTG-regulated promoter (P_{spac}). The Δ*mutS, amyE::*P_{spac}*mutS–gfp* strain was 88.7% functional compared with Δ*mutS, amyE::*P_{spac}*mutS* (Table S1). When either *mutS–gfp* or *mutSF30A–gfp* was ectopically expressed, we observed a two- to threefold increase in the per cent of untreated cells with foci (Fig. 4A, compare with Fig. 2C). This result was not affected by the presence or absence of *mutL*.

We then asked if increased expression of *mutS–gfp* and *mutSF30A–gfp* and the associated mismatch independent foci correlated with colocalization with the replisome marker *dnaX–mcfp*. We found that ectopic expression caused an increase in colocalization to ~ 65%, (Fig. 4B). When these cells were challenged with 2-AP, we expect a decrease in colocalization and indeed found ~ 41% were colocalized following 2-AP challenge (Fig. 4B). Ectopic expression of MutSF30A increased the per cent of cells with foci, and colocalization of MutSF30A, which only forms mismatch-independent foci, remained at ~ 70% upon ectopic expression. These results show that increased expression of MutS increases the percentage of cells with foci colocalized to the replisome (Fig. 4A), supporting the hypothesis that MutS is positioned at the replisome via a binding partner prior to mismatch identification.

It should be noted that in our colocalization experiments we used DnaX as a replisome marker instead of DnaN, which binds MutS *in vitro*, because the *dnaN–mcfp* fusion maintains an elevated mutation rate (25.3×10^{-9} mutations per generation) whereas *dnaX–mcfp* is wild type for mutation rate (data not shown). We determined that the smaller DnaX–mCherry foci colocalizes with DnaN–GFP foci in ~ 89% of cells, establishing DnaX as an appropriate substitute for DnaN in this analysis (Fig. S5).

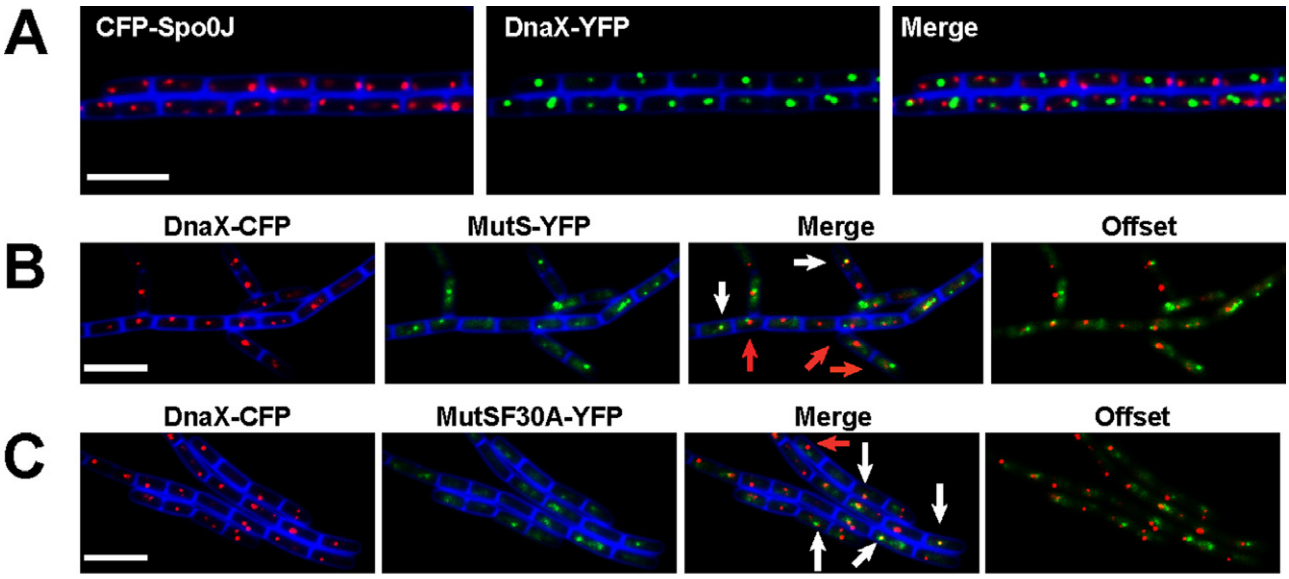

D

Per cent colocalization to DnaX

Fusion	Addition of 2-AP	% colocalization (+/- 95% CI)	No. of cells analysed	
MutS-YFP	-	55.6% (7.7)	160	*
	+	35.5% (5.6)	279	
MutSF30A-YFP	-	73.4% (6.7)	169	** ***
	+	70.1% (8.7)	107	
MutL-GFP	-	58.5% (8.5)	130	#
	+	49.5% (7.1)	190	
CFP-Spo0J	-	12.8% (3.8)	297	

Fig. 3. MutS–GFP colocalizes with the replisome prior to mismatch detection.
A. Representative images of CFP–Spo0J and DnaX–YFP colocalization with the replisome.
B. Representative images of colocalization between MutS–YFP with DnaX–CFP following 2-AP treatment. White arrows denote MutS–YFP foci that colocalize with the DnaX–CFP, whereas red arrows denote MutS–YFP foci that do not colocalize with DnaX–CFP.
C. Representative images of colocalization between MutSF30A–YFP with DnaX–CFP following 2-AP treatment.
The vital membrane stain TMA-DPH is shown in blue, the white bar is 4 μm.
D. Scoring of colocalization of MutS–YFP and MutL–GFP at the replisome in the presence and absence of 2-AP, *P*-values are one-tailed; $P = {}^{*}2.03 \times 10^{-5}$; **2.77; $^{***}4.77 \times 10^{-10}$; #0.0568

MutSF30A–GFP foci are positioned at the replisome by DnaN prior to mismatch binding

The ability of MutSF30A–GFP to assemble into foci without mismatch identification suggests that MutS may be positioned at the replisome as a mechanism to spatially target newly formed mismatches in DNA. Furthermore, colocalization of MutSF30A with the replisome and MutSF30A binding to DnaN *in vitro* (Fig. 1E) suggest that MutSF30A localization is dependent on an interaction with a protein component of the replisome. In *B. subtilis,* DnaN forms large clamp assemblies termed 'clamp zones' that form behind progressing replication forks (Su'etsugu and Errington, 2011). DnaN clamp zones contain ~ 200 accumulated clamps as clamp loading and unloading rates achieve equilibrium (Su'etsugu and Errington, 2011).

We hypothesized that a clamp zone facilitates the formation of mismatch-independent foci by recruiting MutS to the replisome via contact with DnaN. To test this hypothesis, we took advantage of the *dnaN5* allele, which exhibits an increase in mutation frequency due to partial loss of MMR (Simmons *et al*., 2008; Dupes *et al*., 2010; and Table S1). The *dnaN5* allele exhibits a temperature-sensitive defect in MMR, which leads to a significant decrease in MutS–GFP focus formation at 37°C relative to 30°C. We determined that DnaN5 functions normally in DNA replica-

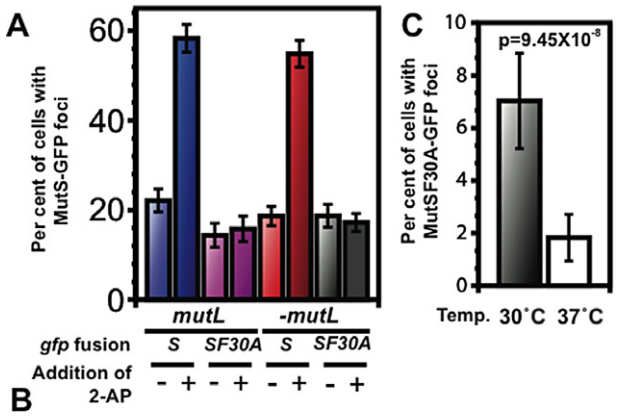

Colocalization following ectopic expressing MutS or MutSF30A-GFP

Genotype	Addition of 2-AP	Per cent of colocalization (95% CI)
ΔmutS, amyE:P$_{spac}$mutS-gfp, dnaX - mCherry	-	65.1 (9.1)
	+	40.8 (6.9)
ΔmutS, amyE:P$_{spac}$mutSF30A-gfp, dnaX - mCherry	-	68.7 (7.1)
	+	70.6 (7.7)

Fig. 4. Elevated expression of MutS–GFP increases replisome-associated foci.
A. Elevated expression of *mutS–gfp* and *mutSF30A–gfp* increases the percentage of cells with MutS foci. The first four groups contain a Δ*mutS* deletion and the expressed GFP fusion represents the sole copy of *mutS* within the cell. The second four groups represent a deletion of the entire *mutSL* locus with *mutS*– or *mutSF30A–GFP* expressed ectopically from a P_{spac} promoter.
B. Elevated expression of *mutS–gfp* causes an increase in colocalization of MutS foci to DnaX–mCherry foci. Total number of cells scored is 106–196.
C. MutSF30A–GFP foci expressed from the *mutS* native locus in the *dnaN5* background at 30°C and 37°C.

tion by measuring replication *in vivo* and found that *dnaN5* is wild type for DNA synthesis and growth rate at both 30°C and 37°C (Fig. S6; Simmons *et al*., 2008; Dupes *et al*., 2010). We introduced *dnaN5* into a strain bearing the *mutSF30A–gfp* allele at its native locus and scored the number of MutSF30A–GFP foci at 30°C and 37°C. At 30°C, we found that ~ 7% of cells contain a MutSF30A–GFP focus, results consistent with that of a *dnaN*$^{+}$ strain (Figs 2C and 4C). In contrast, at 37°C, the percentage of cells with MutSF30A–GFP foci decreased to < 2% ($P = 9.45 \times 10^{-8}$). Three prominent models have been used to explain the role of DnaN in MMR. The first model suggests that MutS is stabilized or mismatch recognition affinity is increased through interaction with the replication clamp (Flores-Rozas *et al*., 2000; Lau and Kolodner, 2003; Simmons *et al*., 2008). The second model primarily supported from studies in human cell culture and *S. cerevisiae* predicts that MutS is recruited to sites of replication (Kleczkowska *et al*., 2001; Hombauer *et al*., 2011a). Finally, the third model suggests that the major role for DnaN clamp is during resynthesis of the DNA (Pluciennik *et al*., 2009). Our data show that interaction with DnaN is critical for formation of the mismatch-independent MutS foci *in vivo*. We further interpret these results to mean that DnaN clamp zones recruit and stage MutS immediately behind the advancing replication forks *in vivo* supporting the model that MutS is recruited to sites of replication before mismatch binding strongly supporting the second model.

DnaN clamp zones increase efficiency of mismatch detection by targeting MutS to nascent DNA

In defined *in vitro* MMR systems, purified MutS and MutSα can detect a mismatch in DNA without the need for a processivity clamp (e.g. Tessmer *et al*., 2008; Zhai and Hingorani, 2010). We hypothesized that the association of MutS with DnaN might be necessary *in vivo* in order to restrict the search for mismatches to nascent DNA, making mismatch detection more efficient relative to MutS identifying a mismatch independent of DnaN binding. To test the key hypothesis that a DnaN clamp zone recruits MutS, we took advantage of the *mutS800* allele, which lacks a C-terminal tether and is defective in DnaN binding, but is proficient for mismatch identification (Simmons *et al*., 2008). When the *B. subtilis mutS800* allele was expressed from its native promoter, only ~ 9.5% of MMR activity is observed *in vivo* (Table 2). The *mutS800* allele can support 97.4% MMR activity when this mutant protein is overex-

Table 2. DnaN allows for efficient mismatch repair (MMR) *in vivo*.

Relevant genotype	No. of cultures	Mutation rate (10^{-9} mutations per generation) ± [95% CI]	Relative mutation rate	Total MMR activity (%)
ΔmutS, amyE::P$_{spac}$mutS	25	3.09 [1.35–4.68]	1	100
ΔmutS	28	159.3 [152.0–166.6]	51.5	0
mutS800	25	144.5 [134.9–154.2]	46.7	9.5
ΔmutS, amyE::P$_{spac}$mutS800	23	7.10 [4.39–9.74]	2.3	97.4

The Δ*mutS* designation indicates an in-frame deletion of *mutS*, maintaining a functional *mutL* at its native locus (see *Experimental procedures*). The *mutS800* allele was expressed from its native locus with *mutL* expressed ectopically from *amyE* using 1 mM IPTG. Brackets enclose the lower bounds and upper bounds of the 95% confidence limits. Per cent MMR activity was determined using the following equation: [(RMRnull – RMRstrain)/(RMRnull – RMRwild type)]•100. RMR = relative mutation rate. Mutations per culture (m) are as follows: *ΔmutS, amyE::P$_{spac}$mutS* (1.78); Δ*mutS* (104.5); *mutS800* (64.2); *ΔmutS, amyE::P$_{spac}$mutS800* (5.0).

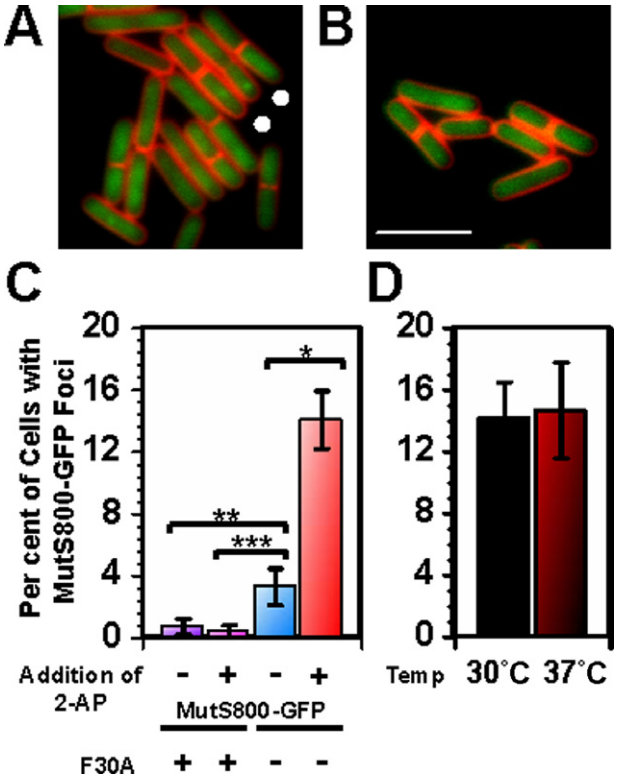

Fig. 5. Mismatch detection by MutS800–GFP induces focus formation at nascent DNA when ectopically expressed.
A. MutS800–GFP foci form in response to mismatches independent of DnaN (faint foci indicated by white circles).
B. MutSF30A800 fails to form foci. The vital membrane stain TMA-DPH is shown in red and the white scale bar is 4 μm.
C. Bar graph of ectopically expressed MutS800–GFP and MutSF30A800–GFP foci with and without 2-AP. From left to right, total cells scored: 1114, 1154, 883, 1343. *P*-values are one-tailed: $*P = 2.69 \times 10^{-17}$, $**P = 1.20 \times 10^{-5}$, $***P = 3.22 \times 10^{-7}$.
D. Bar graph of ectopically expressed MutS800–GFP foci within the *dnaN5* background revealed no statistical difference at 30°C and 37°C ($P = 0.38$).

pressed from an IPTG driven P_{spac} promoter from an ectopic locus in a strain lacking the native *mutS* allele (Table 2). Immunoblotting shows that the P_{spac}*mutS800* protein level was fourfold higher than the level produced from the *mutS800* allele located at the *mutS* native locus (Fig. S7). This result supports the hypothesis that increasing MutS800 concentration can compensate for the loss of interaction with DnaN and restore efficient MMR activity.

When *mutS800–gfp* is expressed from the *mutS* native locus, the protein is defective in forming foci in response to mismatches *in vivo* (Simmons *et al.*, 2008). Since *mutS800* restores MMR activity when ectopically expressed, we asked if *mutS800–gfp* also forms foci following ectopic expression. Upon visualizing ectopically expressed MutS800–GFP in a Δ*mutS* background, we found that MutS800–GFP formed occasional foci in untreated cells (Fig. 5A); however, focus intensity was barely above the elevated background fluorescence and only formed in ~ 3.3% of cells. Upon 2-AP treatment, the percentage of cells with faint foci substantially increased to 14.1%, indicating that like MutS–GFP (Fig. 2), MutS800–GFP focus formation is responsive to an increase in mismatches in DNA. To verify this observation, we asked if mismatch binding by MutS800 was important for focus formation. To answer this question, *mutSF30A800–gfp* was placed under the control of an IPTG driven P_{spac} promoter and inserted at an ectopic locus in a Δ*mutS* background. This allele is defective in both DnaN clamp binding and mismatch detection. We predicted that overexpressed MutSF30A800 would fail to localize into foci if the observed localization of ectopically expressed *mutS800* was dependent on mismatches and independent of DnaN. Indeed, we found that MutSF30A800 was blocked for focus formation (Fig. 5B) (< 1% in both 2-AP-treated and untreated samples). We conclude that when the DnaN tether on MutS is removed, mismatch binding becomes obligatory for focus formation *in vivo* (Fig. 5A–C). We further verified this observation by inserting the *dnaN5* allele into the Δ*mutS, amyE::*P_{spac}*mutS–gfp* background. At both 30°C and 37°C, MutS800–GFP formed foci in ~ 14% of cells, consistent with our results for the *dnaN*$^{+}$ allele (Fig. 4C) and further confirming bypass of the DnaN role in MMR following overexpression (Fig. 5C and D).

Because overexpression of *mutS800* restores MMR to near wild-type levels, bypassing the need for DnaN (Table 2), we asked where ectopically expressed MutS800 foci form *in vivo*. To address this question, we visualized and scored the subcellular location of ectopically expressed MutS800–GFP in comparison with natively expressed MutS–GFP. Upon scoring focus positions in the cell relative to the closest pole, we found that MutS800–GFP foci formed in the same subcellular positions as MutS–GFP foci (Fig. 6A). Moreover, following 2-AP challenge, MutS800–GFP colocalizes with DnaX–mCherry to almost the same extent as wild-type MutS–GFP (Fig. 6B, 29.9 ± 6.28% for MutS800–GFP and 35.5 ± 5.6 for MutS–GFP: $P = 0.099$). Finally, the vast majority of foci that do not colocalize with the replisome are replisome proximal (Fig. 6C). These results indicate that ectopically expressed MutS800–GFP also localizes to replisome proximal DNA for mismatch detection and initiation of repair; however, as shown previously, higher amounts of this mutant protein are required to achieve the same level of MMR as wild-type MutS (Table 2 and Fig. S7). Thus, MMR in *B. subtilis* is initiated and occurs predominantly in replisome proximal regions of DNA, and association of MutS with DnaN increases the efficiency of mismatch detection and repair by targeting MutS to nascent DNA. When DnaN-mediated mismatch detection is bypassed, as with MutS800 following overexpression, we found that MutS800 still forms foci in replisome proximal

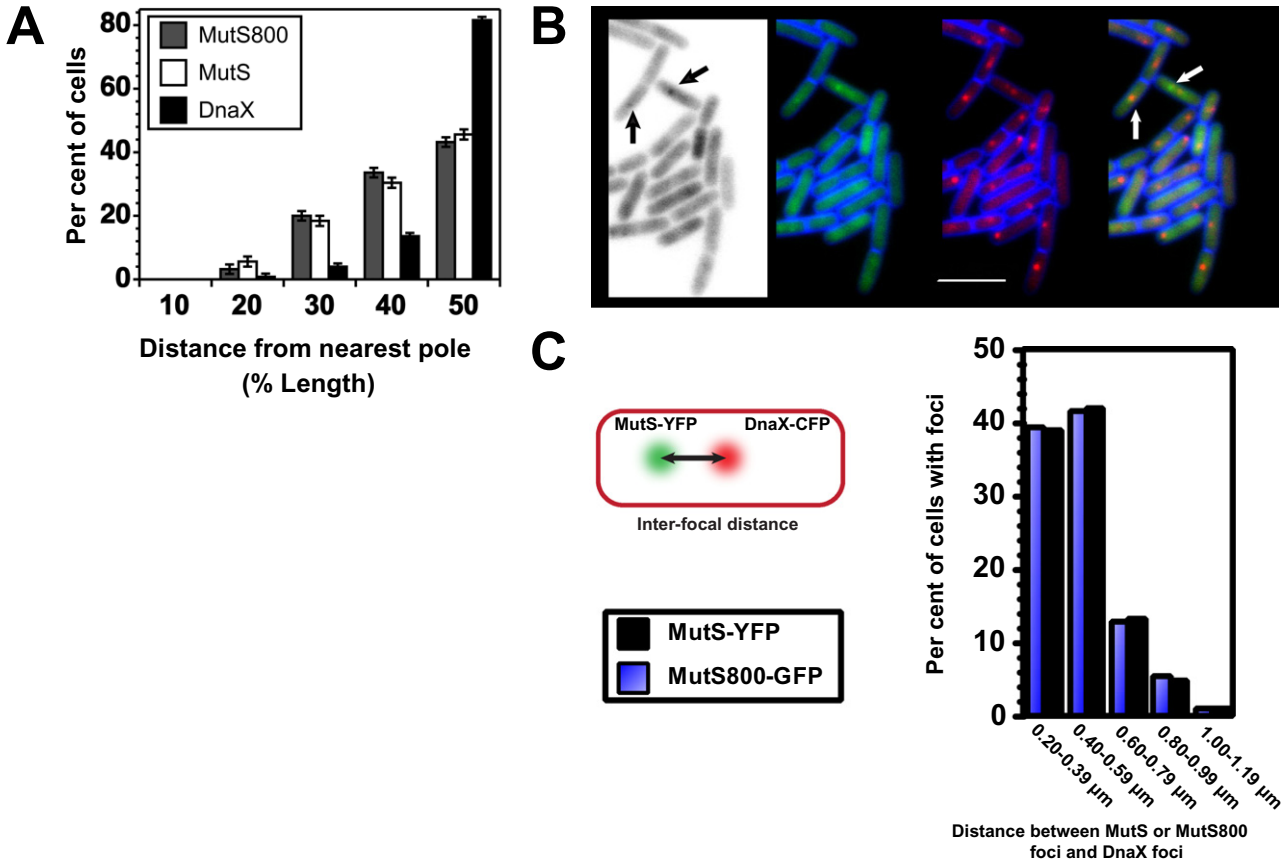

Fig. 6. DnaN-independent focus formation of MutS800–GFP localizes to the same subcellular position as MutS–YFP.
A. Position of MutS–GFP, ectopically expressed MutS800–GFP and DnaX–GFP foci scored relative to cell length ($n = 125$ cells for each group).
B. 29.9 + 6.3% ($n = 204$) of the MutS800–GFP colocalizes with DnaX–mCherry. These results are not statistically different with $P = 0.099$ when compared with MutS–YFP colocalization with DnaX–CFP 35.5 + 5.6 shown in Fig. 3. The left most image is the negative image, MutS800–GFP, DnaX–mCherry and a merge. The membrane is stained with TMA-DPH and is shown in blue, and the scale bar represents 4 μm.
C. We measured the inter-focal distance (IFD) between MutS–YFP and MutS800–GFP foci that failed to colocalize with DnaX–mCherry foci. No IFDs were measured less than 0.2 μm. We measured 94 MutS800–GFP, DnaX–mCherry and 105 MutS–YFP, DnaX–CFP focal pairs that failed to colocalize. Each bar represents the percentage of cells with IFD between the indicated distance.

DNA *in vivo* (see *Discussion*). Together, our results show that in order to initiate MMR, MutS must localize to the replisome or at least near the replisome in *B. subtilis*.

Discussion

Three current models are used to explain the role of processivity clamps in MMR: clamps stabilize MutS at a mismatch or increase mismatch binding affinity (Flores-Rozas *et al.*, 2000; Lau and Kolodner, 2003; Simmons *et al.*, 2008), clamps recruit MutS to sites of DNA replication (Kleczkowska *et al.*, 2001; Hombauer *et al.*, 2011a) or that clamps are required for DNA synthesis (Pluciennik *et al.*, 2009). We have shown in this study that the *B. subtilis* processivity clamp, DnaN, facilitates ~ 90% of MMR and targets MutS to replisome proximal DNA prior to mismatch binding. A DnaN clamp zone forms in the wake of active replication forks (Su'etsugu and Errington, 2011), providing a platform for MutS to maintain a critical spatial and temporal relationship with the replisome (Fig. 7). We propose that DnaN-mediated targeting of MutS to nascent DNA allows for efficient mismatch detection by allowing for MutS to target newly formed errors.

MutS homologues spanning bacteria to humans exhibit the near-ubiquitous presence of a clamp-binding motif, suggesting that association with processivity clamps is important for MMR (Dalrymple *et al.*, 2001). It has been known for decades that MutS is able to detect mismatches without accessory factors *in vitro* (e.g. Su and Modrich, 1986; Prolla *et al.*, 1994; Acharya *et al.*, 1996). Nevertheless MutS800, which lacks the DnaN clamp-binding tether, is largely inactive for MMR while under control of its native promoter, retaining less than 10% activity. Interestingly, the same *mutS800* allele restored

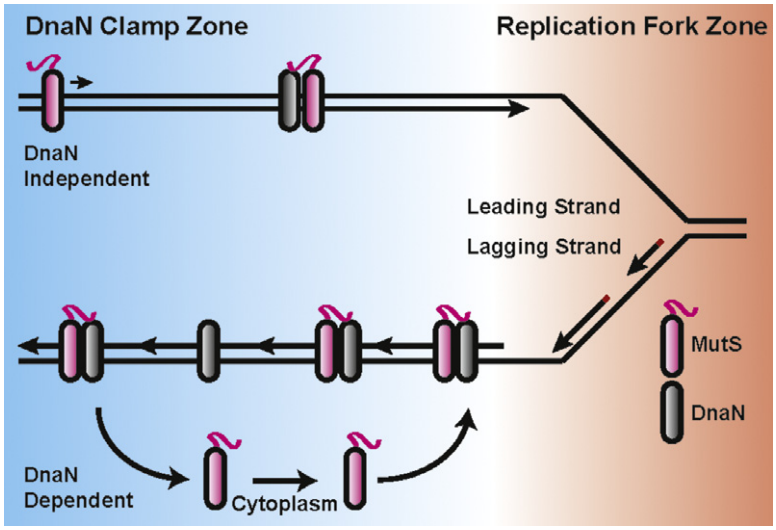

Fig. 7. Model for temporal coupling of MutS to DNA replication. MutS relies on a DnaN clamp zone to target MutS to nascent DNA. DnaN-dependent mode of mismatch detection represents 90% of repair. This figure is adapted from the clamp zone model (Su'etsugu and Errington, 2011).

MMR activity to 97% *in vivo* upon overexpression. Our finding that MutS800 is capable of mismatch detection in the absence of DnaN *in vivo* led us to speculate that MutS800 could find mismatches and initiate repair at chromosomal locations distal to the replisome. To the contrary, we found that ectopically expressed MutS800–GFP formed foci at virtually identical subcellular positions as MutS–GFP, while MutSF30A800–GFP, which cannot bind mismatches or DnaN, was completely defective for focus formation. This result demonstrates that MutS800 binds mismatches in a replisome-proximal position like wild-type MutS; however, an approximately fourfold increase in concentration of the mutant protein is required to restore mismatch detection efficiency and compensate for the loss of interaction with DnaN. It was shown previously that *B. subtilis* MutL binds DnaN, and disruption of this contact causes complete loss of MMR *in vivo* (Pillon *et al*., 2010; 2011). Overexpression of MutL mutants defective in binding DnaN fail to bypass the need for interaction with DnaN during MMR (Pillon *et al*., 2010; 2011). We propose that MutS800 must identify mismatches in replisome proximal DNA to enable the downstream steps of repair, which include MutL recruitment and activation of its endonuclease activity. Current data suggest that these steps are dependent on interaction with DnaN, and may therefore require MutS to bind mismatches in the DnaN clamp zone in order to complete the downstream steps of MMR (Pillon *et al*., 2010; 2011).

Consistent with our findings, in *Escherichia coli*, when *mutS800* is expressed from its native promoter, it confers an MMR defect, but is close to wild type for MMR when overexpressed from a plasmid (Lamers *et al*., 2000; Calmann *et al*., 2005). Similarly, the equivalent mutant in *Pseudomonas aeruginosa*, *mutS798*, complements a *mutS*-deficient strain when overexpressed from a plasmid (Monti *et al*., 2012). Thus, in these systems, MutS is also capable of operating independent of DnaN, since both *P. aeruginosa* MutS798 and *E. coli* MutS800 fail to bind their cognate DnaN clamps (Calmann *et al*., 2005; Lopez de Saro *et al*., 2006; Monti *et al*., 2012). We propose that in these bacteria, when MutS is present at wild-type levels, interaction with DnaN is important for targeting MMR to nascent DNA. When the protein is overexpressed, the requirement for DnaN is bypassed due to the increased likelihood of MutS directly binding mismatches in nascent DNA without DnaN association.

The model of a DnaN clamp zone that facilitates spatial and temporal coupling of mismatch detection with replication is an intriguing one, especially when considering the conservation of processivity clamp-binding motifs in MutS homologues (Flores-Rozas *et al*., 2000; Dalrymple *et al*., 2001). Consistent with the clamp zone model, fluorophore-labelled processivity clamps form foci *in vivo* in bacteria and eukaryotes (e.g. Kleczkowska *et al*., 2001; Hombauer *et al*., 2011a), suggesting that substantial local concentrations of clamps are present in organisms other than *B. subtilis*. The observation that a PCNA clamp zone may exist also agrees well with the higher proficiency of MMR on the lagging strand relative to the leading strand in *S. cerevisiae* (Pavlov *et al*., 2003). Other *B. subtilis* studies have shown that DnaN clamps are competent for protein recruitment to nascent DNA *in vivo*, as fluorophore-labelled peptides encoding a DnaN-binding motif are sufficient for forming replisome-localized foci (Simmons *et al*., 2008; Su'etsugu and Errington, 2011). A similar finding was reported for *S. cerevisiae*. When *msh6 305–1242*Δ, the unstructured region of *msh6* that contains the PIP motif for binding PCNA (^{27}-**QSSLLSFF**-^{34}), was expressed from the native *msh6* promoter this region was sufficient to form foci (Hombauer *et al*., 2011a). Furthermore, in human cell culture,

overexpression of either MSH6 or MSH3 (which contain PIP motifs ^{4}**Q**ST**L**YS**FF**-^{11} and ^{21}-**Q**AV**L**SR**FF**-^{28} respectively) resulted in colocalization of MutSα and MutSβ with both PCNA and BrdU stain (Kleczkowska *et al*., 2001). Truncating the N-terminal 77 residues of MSH6 eliminated both MSH6 binding to PCNA *in vitro* and focus formation *in vivo*, indicating that localization of human MutS homologues to nascent DNA is dependent on interaction with PCNA (Kleczkowska *et al*., 2001). Collectively, these results support the hypothesis that a PCNA clamp zone present at nascent DNA facilitates mismatch detection *in vivo*. Our data further agree well with the observation that MMR must occur concurrently with DNA replication in *S. cerevisiae* (Hombauer *et al*., 2011b). It was recently reported in *S. cerevisiae* that PCNA-dependent MMR accounts for only 10–15% of MMR (Hombauer *et al*., 2011a), whereas DnaN-dependent MMR in *B. subtilis* accounts for ~ 90% of MMR by MutS. This is a notable difference in the orchestration of MMR between these organisms *in vivo*.

Another important finding from our study is that MutS localizes near the replisome independent of mismatch identification through the DnaN clamp zone. This conclusion is based on the observation that MutSF30A also forms foci that colocalize with the replisome, despite its inability to bind mismatches. Moreover, the MMR compromised *dnaN5* mutant nearly abolishes MutSF30A–GFP localization in *B. subtilis*, indicating that MutSF30A foci are dependent on interaction with DnaN. Based on these data, we propose that MutS is coupled with the progressing replication fork prior to mismatch identification. An additional important finding is that after detecting a mismatch, MutS detaches from the replisome (DnaN) and remains at the mismatch site to conduct repair. This conclusion is based on the observation that MutS–YFP colocalizes less frequently with the replisome in 2-AP-treated cells. Moreover, overexpression of MutS–YFP increases colocalization to the replisome in untreated cells, but there is little increase in colocalization following 2-AP treatment. Finally, the frequency of MutSF30A colocalization with the replisome is unchanged following 2-AP treatment, again, supporting the hypothesis that binding to mismatches causes release of MutS from the replisome. Overall, this study shows that MutS foci represent assemblies undergoing active repair of replication errors with two distinctive steps clearly identified: DnaN-coupled targeting of MutS to nascent DNA and release of MutS from the replisome following mismatch recognition.

Experimental procedures

Bacteriological methods

All *B. subtilis* strains (Table S2) are isogenic derivatives of PY79 and grown according to standard procedures (Hardwood and Cutting, 1990). All oligos used in this study are listed in Table S3. To determine relative mutation rate, *B. subtilis* cells were grown at 37°C to OD_{600} of ~ 1.2, concentrated and resuspended in 100 µl of 0.85% saline. A portion of the cells was serial diluted (10^{-6}) and plated onto LB agar plates to determine the total viable count within the culture. The remaining resuspension was plated onto LB agar plates supplemented with 150 µg ml^{-1} rifampin. Mutation rate analysis was performed using MSS Maximum Likelihood Method with the 95% confidence interval, and statistical significance assessed using a one- or two-tailed *t*-test (Foster, 2006; Hall *et al*., 2009; Bolz *et al*., 2012).

Epifluorescence microscopy

Cells were prepared for live cell imaging essentially as described (Simmons *et al*., 2007; 2009; Klocko *et al*., 2010). Briefly, strains were inoculated to a starting OD_{600} in $S7_{50}$ minimal media supplemented with 2% D-glucose. Cells were grown past three doublings to an OD_{600} of 0.4–0.5 and were split: one control culture and one culture challenged with 2-aminopurine to a final concentration of 600 µg ml^{-1} for 1 h. Cell membranes were visualized using the fluorescent probe TMA-DPH at a working concentration of 10 µM. Replisome fusions were imaged with 0.5–1.0 s exposures while MMR fusion proteins were imaged at 1.2–2.5 s exposures. Scoring of cells as containing a MutS focus is outlined in Fig. S8. The average cell focus encompasses ~ 4% of the cell area with an average intensity twofold greater than background. Colocalization and localization experiments were conducted as above except cells were grown in $S7_{50}$ minimal media supplemented with 1% L-arabinose. These conditions were used to produce cells with predominantly 1 DnaX–GFP focus per cell (average is 1.72 foci per cell with 39.1% of cells containing one focus) (Fig. S3). Image capture of both fusion proteins during colocalization experiments was performed in immediate succession and timed < 2 s of total capture to minimize any intracellular movement of either the MutS or replisomal fusions. For temperature release experiments, cells were grown and treated as above, but the prepared slide was incubated for 15 min at indicated temperature. Upon removal from the temperature-regulated chamber, slides were imaged for 5 min immediately upon removal.

Statistical analysis

Bar graphs are presented with error bars representing the 95% confidence interval, and statistical significance was determined using a one- or two-tailed *t*-test.

Immunoblotting

Bacillus subtilis whole-cell extracts were obtained basically as described (Rokop *et al*., 2004). Briefly, mid-exponential phase cultures were centrifuged and lysed by sonication (20 Hz), resuspended in lysis buffer [10 mM Tris-HCl (pH 7.0), 0.5 mM EDTA, 1 mM AEBSF and 1× Protease Inhibitor Cocktail (Thermo Scientific)], and protein concentration was determined using Pierce BCA Protein Assay Kit (Thermo Scientific). Equal amounts of total protein were

applied to each lane on a 4–15% gradient gel, and protein levels were probed with purified antisera: α-MutS (MI-1042), α-MutL (MI-1044) and α-DnaN (MI-1039). Immunoblots were developed as described previously (Simmons and Kaguni, 2003).

Immunodot blotting

Immunodot blotting was performed as previously described (Klocko *et al.*, 2011; Walsh *et al.*, 2012). Briefly, indicated proteins were immobilized onto a nitrocellulose membrane with the assistance of a Bio-dot microfiltration apparatus (Bio-Rad). The membrane was incubated in blocking buffer (5% dry non-fat milk, 17.4 mM Na_2HPO_4, 2.6 mM NaH_2PO_4, 150 mM NaCl, 0.05% Tween-20) at 22°C for 1 h. All subsequent washes and incubations took place in blocking buffer. After blocking, the membrane was incubated with 0.4 μM DnaN in blocking buffer for 3 h at 22°C. The blot was subsequently washed three times and then incubated with affinity-purified α-DnaN antisera overnight at 4°C. The blot was removed from primary antibody (MI 1038) and washed three times at 22°C and placed in secondary antisera (1:2000 α-Rabbit) for 2 h at 22°C. The blot was washed three more times, followed by a wash in PBS (17.4 mM Na_2HPO_4, 2.6 mM NaH_2PO_4, 150 mM NaCl, 0.05% Tween-20) to remove excess milk proteins. The membrane was developed with chemiluminescence (Super-Signal Altra, Pierce) and expose to film as described (Klocko *et al.*, 2011).

B. subtilis *MutS–DNA interactions at equilibrium*

Procedures used to purify untagged MutS and MutSF30A are detailed within the supplemental methods.

The mismatched DNA substrates for the MutS–DNA binding assay were prepared by annealing 37 nt 2-aminopurine (2-AP) labelled +T strand (5′-TAA AGG AAG TCG TCT AT2-Ap *T*AT GGT ATG ACT AAG TGT A-3′) with 36 nt (5′-T ACA CTT AGT CAT ACC AT TAT AGA CGA CTT CCT TTA-3′) or with 37 nt (5′-T ACA CTT AGT CAT ACC ATG TAT AGA CGA CTT CCT TTA-3′) strands to yield 2-AP(+T) and 2-AP(GT) duplexes respectively. The matched substrate, 2-AP(GC) was prepared by annealing 37 nt 2-AP labelled strand (5′-TAA AGG AAG TCG TCT AT2-Ap CAT GGT ATG ACT AAG TGT A-3′) with a 37 nt strand (5′-T ACA CTT AGT CAT ACC ATG TAT AGA CGA CTT CCT TTA-3′). The strands were heated to 95°C, followed by slowly cooling to room temperature to obtain annealed duplex DNAs.

DNA binding was measured on a FluoroMax-3 fluorimeter (Jobin-Yvon Horiba Group; Edison, NJ). Titrations of 0.02 μM 2-AP(+T), 2-AP(GC) and 2-AP(GT) duplex DNAs with 0–0.4 μM MutS were performed in 3 ml quartz cuvettes in DNA binding buffer (20 mM Tris-HCl, pH 7.6, 50 mM NaCl, 5 mM $MgCl_2$) at 25°C. MutS was added incrementally to the sample, and fluorescence intensity was measured after mixing for 30 s ($\lambda_{EX} = 315$ nm and $\lambda_{EM} = 375$ nm). The data were corrected for intrinsic MutS fluorescence by subtracting data from parallel experiments with unlabelled DNA. Fluorescence intensity was plotted versus MutS concentration and the apparent dissociation constant (K_D) for the interaction was obtained by fitting the data to a quadratic equation:

$$[D \cdot M] = F_0 + (F_{max} - F_0)\{[(K_D + [D_t] + [M_t]) - [(K_D + [D_t] + [M_t])^2 - 4[D_t][M_t]]^{1/2}]/2[D_t]\}$$

where $D{\cdot}M$ is the fraction of MutS•DNA, F_0 is 2-AP(+T) fluorescence in the absence of protein and F_{max} is maximal fluorescence, and D_t and M_t are total molar concentrations of DNA and MutS respectively. The data were fit by non-linear regression using KaleidaGraph (Synergy Software).

Acknowledgements

We thank Dr David Rudner (Harvard Medical School) and Dr Heath Murray (Newcastle University) for strains. We would like to thank members of the Simmons lab for critical reading of this manuscript and the comments from two anonymous referees. This work was supported by grants from the Wendy Will Case Cancer Fund to L.A.S. and grants from the National Science Foundation to L.A.S. (MCB 1050948) and M.M.H. (MCB 1022203).

References

Acharya, S., Wilson, T., Gradia, S., Kane, M.F., Guerrette, S., Marsischky, G.T., *et al.* (1996) hMSH2 forms specific mispair-binding complexes with hMSH3 and hMSH6. *Proc Natl Acad Sci USA* **93:** 13629–13634.

Alani, E., Chi, N.W., and Kolodner, R. (1995) The *Saccharomyces cerevisiae* Msh2 protein specifically binds to duplex oligonucleotides containing mismatched DNA base pairs and insertions. *Genes Dev* **9:** 234–247.

Berkmen, M.B., and Grossman, A.D. (2006) Spatial and temporal organization of the *Bacillus subtilis* replication cycle. *Mol Microbiol* **62:** 57–71.

Bolz, N.J., Lenhart, J.S., Weindorf, S.C., and Simmons, L.A. (2012) Residues in the N-terminal domain of MutL required for mismatch repair in *Bacillus subtilis*. *J Bacteriol* **194:** 5361–5367.

Bowers, J., Tran, P.T., Liskay, R.M., and Alani, E. (2000) Analysis of yeast MSH2–MSH6 suggests that the initiation of mismatch repair can be separated into discrete steps. *J Mol Biol* **302:** 327–338.

Bowman, G.D., O'Donnell, M., and Kuriyan, J. (2004) Structural analysis of a eukaryotic sliding DNA clamp–clamp loader complex. *Nature* **429:** 724–730.

Calmann, M.A., Nowosielska, A., and Marinus, M.G. (2005) The MutS C terminus is essential for mismatch repair activity *in vivo*. *J Bacteriol* **187:** 6577–6579.

Chopra, I., O'Neill, A.J., and Miller, K. (2003) The role of mutators in the emergence of antibiotic-resistant bacteria. *Drug Resist Updat* **6:** 137–145.

Clark, A.B., Valle, F., Drotschmann, K., Gary, R.K., and Kunkel, T.A. (2000) Functional interaction of proliferating cell nuclear antigen with MSH2–MSH6 and MSH2–MSH3 complexes. *J Biol Chem* **275:** 36498–36501.

Cooper, L.A., Simmons, L.A., and Mobley, H.L. (2012) Involvement of mismatch repair in the reciprocal control of motility and adherence of uropathogenic *Escherichia coli*. *Infect Immun* **80:** 1969–1979.

Cox, E.C., Degnen, G.E., and Scheppe, M.L. (1972) Mutator

gene studies in *Escherichia coli*: the *mutS* gene. *Genetics* **72:** 551–567.
Culligan, K.M., Meyer-Gauen, G., Lyons-Weiler, J., and Hays, J.B. (2000) Evolutionary origin, diversification and specialization of eukaryotic MutS homolog mismatch repair proteins. *Nucleic Acids Res* **28:** 463–471.
Dalrymple, B.P., Kongsuwan, K., Wijffels, G., Dixon, N.E., and Jennings, P.A. (2001) A universal protein–protein interaction motif in the eubacterial DNA replication and repair systems. *Proc Natl Acad Sci USA* **98:** 11627–11632.
Davies, B.W., Bogard, R.W., Dupes, N.M., Gerstenfeld, T.A., Simmons, L.A., and Mekalanos, J.J. (2011) DNA damage and reactive nitrogen species are barriers to *Vibrio cholerae* colonization of the infant mouse intestine. *PLoS Pathog* **7:** e1001295.
Denamur, E., Bonacorsi, S., Giraud, A., Duriez, P., Hilali, F., Amorin, C., *et al*. (2002) High frequency of mutator strains among human uropathogenic *Escherichia coli* isolates. *J Bacteriol* **184:** 605–609.
Dupes, N.M., Walsh, B.W., Klocko, A.D., Lenhart, J.S., Peterson, H.L., Gessert, D.A., *et al*. (2010) Mutations in the *Bacillus subtilis* beta clamp that separate its roles in DNA replication from mismatch repair. *J Bacteriol* **192:** 3452–3463.
Fishel, R., Lescoe, M.K., Rao, M.R.S., Copeland, N.G., Jenkins, N.A., Garber, J., *et al*. (1993) The human mutator gene homolog *MSH2* and its association with hereditary nonpolyposis cancer. *Cell* **75:** 1027–1038.
Flores-Rozas, H., Clark, D., and Kolodner, R.D. (2000) Proliferating cell nuclear antigen and Msh2p–Msh6p interact to form an active mispair recognition complex. *Nat Genet* **26:** 375–378.
Foster, P.L. (2006) Methods for determining spontaneous mutation rates. *Methods Enzymol* **409:** 195–213.
Georgescu, R.E., Kim, S.S., Yurieva, O., Kuriyan, J., Kong, X., and O'Donnell, M. (2008) Structure of a sliding clamp on DNA. *Cell* **132:** 43–54.
Ginetti, F., Perego, M., Albertini, A.M., and Galizzi, A. (1996) *Bacillus subtilis mutS mutL* operon: identification, nucleotide sequence and mutagenesis. *Microbiology* **142** (Part 8)**:** 2021–2029.
Gruber, S., and Errington, J. (2009) Recruitment of condensin to replication origin regions by ParB/SpoOJ promotes chromosome segregation in *B. subtilis*. *Cell* **137:** 685–696.
Gu, L., Hong, Y., McCulloch, S., Watanabe, H., and Li, G.M. (1998) ATP-dependent interaction of human mismatch repair proteins and dual role of PCNA in mismatch repair. *Nucleic Acids Res* **26:** 1173–1178.
Habraken, Y., Sung, P., Prakash, L., and Prakash, S. (1996) Binding of insertion/deletion DNA mismatches by the heterodimer of yeast mismatch repair proteins MSH2 and MSH3. *Curr Biol* **6:** 1185–1187.
Hall, B.M., Ma, C.X., Liang, P., and Singh, K.K. (2009) Fluctuation analysis CalculatOR: a web tool for the determination of mutation rate using Luria-Delbruck fluctuation analysis. *Bioinformatics* **25:** 1564–1565.
Hamilton, S.R., Liu, B., Parsons, R.E., Papadopoulos, N., Jen, J., Powell, S.M., *et al*. (1995) The molecular basis of Turcot's syndrome. *N Engl J Med* **332:** 839–847.
Hardwood, C.R., and Cutting, S.M. (1990) *Molecular Biological Methods for Bacillus*. Chichester: John Wiley & Sons.
Hombauer, H., Campbell, C.S., Smith, C.E., Desai, A., and Kolodner, R.D. (2011a) Visualization of eukaryotic DNA mismatch repair reveals distinct recognition and repair intermediates. *Cell* **147:** 1040–1053.
Hombauer, H., Srivatsan, A., Putnam, C.D., and Kolodner, R.D. (2011b) Mismatch repair, but not heteroduplex rejection, is temporally coupled to DNA replication. *Science* **334:** 1713–1716.
Huang, C.C., Hearst, J.E., and Alberts, B.M. (1981) Two types of replication proteins increase the rate at which T4 DNA polymerase traverses the helical regions in a single-stranded DNA template. *J Biol Chem* **256:** 4087–4094.
Iyer, R.R., Pluciennik, A., Burdett, V., and Modrich, P.L. (2006) DNA mismatch repair: functions and mechanisms. *Chem Rev* **106:** 302–323.
Jackson, D., Wang, X., and Rudner, D.Z. (2012) Spatio-temporal organization of replication in bacteria and eukaryotes (nucleoids and nuclei). *Cold Spring Harb Perspect Biol* **4:** 1–14.
Jacobs-Palmer, E., and Hingorani, M.M. (2007) The effects of nucleotides on MutS–DNA binding kinetics clarify the role of MutS ATPase activity in mismatch repair. *J Mol Biol* **366:** 1087–1098.
Jeruzalmi, D., O'Donnell, M., and Kuriyan, J. (2001) Crystal structure of the processivity clamp loader gamma (gamma) complex of *E. coli* DNA polymerase III. *Cell* **106:** 429–441.
Kadyrov, F.A., Dzantiev, L., Constantin, N., and Modrich, P. (2006) Endonucleolytic function of MutLalpha in human mismatch repair. *Cell* **126:** 297–308.
Kleczkowska, H.E., Marra, G., Lettieri, T., and Jiricny, J. (2001) hMSH3 and hMSH6 interact with PCNA and colocalize with it to replication foci. *Genes Dev* **15:** 724–736.
Klocko, A.D., Crafton, K.M., Walsh, B.W., Lenhart, J.S., and Simmons, L.A. (2010) Imaging mismatch repair and cellular responses to DNA damage in *Bacillus subtilis*. *J Vis Exp* **36:** 1–4.
Klocko, A.D., Schroeder, J.W., Walsh, B.W., Lenhart, J.S., Evans, M.L., and Simmons, L.A. (2011) Mismatch repair causes the dynamic release of an essential DNA polymerase from the replication fork. *Mol Microbiol* **82:** 648–663.
Kong, X.-P., Onrust, R., O'Donnell, M., and Kuriyan, J. (1992) Three-dimensional structure of the β subunit of *E. coli* DNA polymerase III holoenzyme: a sliding DNA clamp. *Cell* **69:** 425–437.
Krishna, T.S.R., Kong, X.-P., Gary, S., Burgers, P.M., and Kuriyan, J. (1994) Crystal structure of the eukaryotic DNA polymerase processivity factor PCNA. *Cell* **79:** 1233–1243.
Kunkel, T.A. (1992) DNA replication fidelity. *J Biol Chem* **267:** 18251–18254.
Kunkel, T.A., and Bebenek, K. (2000) DNA replication fidelity. *Annu Rev Biochem* **69:** 497–529.
Kunkel, T.A., and Erie, D.A. (2005) DNA mismatch repair. *Annu Rev Biochem* **74:** 681–710.
Lahue, R.S., Au, K.G., and Modrich, P. (1989) DNA mismatch correction in a defined system. *Science* **245:** 160–164.
Lamers, M.H., Perrakis, A., Enzlin, J.H., Winterwerp, H.H., de Wind, N., and Sixma, T.K. (2000) The crystal structure of DNA mismatch repair protein MutS binding to a G × T mismatch. *Nature* **407:** 711–717.
Larrea, A.A., Lujan, S.A., and Kunkel, T.A. (2010) SnapShot: DNA mismatch repair. *Cell* **141:** 730.e1.

Lau, P.J., and Kolodner, R.D. (2003) Transfer of the MSH2·MSH6 complex from proliferating cell nuclear antigen to mispaired bases in DNA. *J Biol Chem* **278:** 14–17.

Lee, S.D., and Alani, E. (2006) Analysis of interactions between mismatch repair initiation factors and the replication processivity factor PCNA. *J Mol Biol* **355:** 175–184.

Lemon, K.P., and Grossman, A.D. (1998) Localization of bacterial DNA polymerase: evidence for a factory model of replication. *Science* **282:** 1516–1519.

Lenhart, J.S., Schroeder, J.W., Walsh, B.W., and Simmons, L.A. (2012) DNA repair and genome maintenance in *Bacillus subtilis*. *Microbiol Mol Biol Rev* **76:** 530–564.

Lopez de Saro, F.J., Marinus, M.G., Modrich, P., and O'Donnell, M. (2006) The beta sliding clamp binds to multiple sites within MutL and MutS. *J Biol Chem* **281:** 14340–14349.

Malkov, V.A., Biswas, I., Camerini-Otero, R.D., and Hsieh, P. (1997) Photocross-linking of the NH2-terminal region of Taq MutS protein to the major groove of a heteroduplex DNA. *J Biol Chem* **272:** 23811–23817.

Matsumiya, S., Ishino, Y., and Morikawa, K. (2001) Crystal structure of an archaeal DNA sliding clamp: proliferating cell nuclear antigen from *Pyrococcus furiosus*. *Protein Sci* **10:** 17–23.

Mena, A., Smith, E.E., Burns, J.L., Speert, D., Moskowitz, S.M., Perez, J.L., and Oliver, A. (2008) Genetic adaptation of *Pseudomonas aeruginosa* to the airways of cystic fibrosis patients is catalyzed by hypermutation. *J Bacteriol* **190:** 7910–7917.

Migocki, M.D., Lewis, P.J., Wake, R.G., and Harry, E.J. (2004) The midcell replication factory in *Bacillus subtilis* is highly mobile: implications for coordinating chromosome replication with other cell cycle events. *Mol Microbiol* **54:** 452–463.

Monti, M.R., Miguel, V., Borgogno, M.V., and Argarana, C.E. (2012) Functional analysis of the interaction between the mismatch repair protein MutS and the replication processivity factor beta clamp in *Pseudomonas aeruginosa*. *DNA Repair (Amst)* **11:** 463–469.

Nystrom-Lahti, M., Perrera, C., Raschle, M., Panyushkina-Seiler, E., Marra, G., Curci, A., *et al*. (2002) Functional analysis of MLH1 mutations linked to hereditary nonpolyposis colon cancer. *Genes Chromosomes Cancer* **33:** 160–167.

Obmolova, G., Ban, C., Hsieh, P., and Yang, W. (2000) Crystal structures of mismatch repair protein MutS and its complex with a substrate DNA. *Nature* **407:** 703–710.

Oliver, A., and Mena, A. (2010) Bacterial hypermutation in cystic fibrosis, not only for antibiotic resistance. *Clin Microbiol Infect* **16:** 798–808.

Oliver, A., Canton, R., Campo, P., Baquero, F., and Blazquez, J. (2000) High frequency of hypermutable *Pseudomonas aeruginosa* in cystic fibrosis lung infection. *Science* **288:** 1251–1254.

Palombo, F., Iaccarino, I., Nakajima, E., Ikejima, M., Shimada, T., and Jiricny, J. (1996) hMutSbeta, a heterodimer of hMSH2 and hMSH3, binds to insertion/deletion loops in DNA. *Curr Biol* **6:** 1181–1184.

Pavlov, Y.I., Mian, I.M., and Kunkel, T.A. (2003) Evidence for preferential mismatch repair of lagging strand DNA replication errors in yeast. *Curr Biol* **13:** 744–748.

Peltomaki, P. (2005) Lynch syndrome genes. *Fam Cancer* **4:** 227–232.

Pillon, M.C., Lorenowicz, J.J., Uckelmann, M., Klocko, A.D., Mitchell, R.R., Chung, Y.S., *et al*. (2010) Structure of the endonuclease domain of MutL: unlicensed to cut. *Mol Cell* **39:** 145–151.

Pillon, M.C., Miller, J.H., and Guarne, A. (2011) The endonuclease domain of MutL interacts with the beta sliding clamp. *DNA Repair (Amst)* **10:** 87–93.

Pluciennik, A., Burdett, V., Lukianova, O., O'Donnell, M., and Modrich, P. (2009) Involvement of the beta clamp in methyl-directed mismatch repair *in vitro*. *J Biol Chem* **284:** 32782–32791.

Pluciennik, A., Dzantiev, L., Iyer, R.R., Constantin, N., Kadyrov, F.A., and Modrich, P. (2010) PCNA function in the activation and strand direction of MutLalpha endonuclease in mismatch repair. *Proc Natl Acad Sci USA* **107:** 16066–16071.

Prolla, T.A., Pang, Q., Alani, E., Kolodner, R.D., and Liskay, R.M. (1994) MLH1, PMS1, and MSH2 interactions during the initiation of DNA mismatch repair in yeast. *Science* **265:** 1091–1093.

Prudhomme, M., Martin, B., Mejean, V., and Claverys, J. (1989) Nucleotide sequence of the *Streptococcus pneumoniae hexB* mismatch repair gene: homology of *HexB* to *MutL* of *Salmonella typhimurium* and to *PMS1* of *Saccharomyces cerevisiae*. *J Bacteriol* **171:** 5332–5338.

Prunier, A.L., Malbruny, B., Laurans, M., Brouard, J., Duhamel, J.F., and Leclercq, R. (2003) High rate of macrolide resistance in *Staphylococcus aureus* strains from patients with cystic fibrosis reveals high proportions of hypermutable strains. *J Infect Dis* **187:** 1709–1716.

Rokop, M.E., Auchtung, J.M., and Grossman, A.D. (2004) Control of DNA replication initiation by recruitment of an essential initiation protein to the membrane of *Bacillus subtilis*. *Mol Microbiol* **52:** 1757–1767.

Roman, F., Canton, R., Perez-Vazquez, M., Baquero, F., and Campos, J. (2004) Dynamics of long-term colonization of respiratory tract by *Haemophilus influenzae* in cystic fibrosis patients shows a marked increase in hypermutable strains. *J Clin Microbiol* **42:** 1450–1459.

Sanjanwala, B., and Ganesan, A.T. (1991) Genetic structure and domains of DNA polymerase III of *Bacillus subtilis*. *Mol Gen Genet* **226:** 467–472.

Schaaper, R.M. (1993) Base selection, proofreading, and mismatch repair during DNA replication in *Escherichia coli*. *J Biol Chem* **268:** 23762–23765.

Schofield, M.J., and Hsieh, P. (2003) DNA mismatch repair: molecular mechanisms and biological function. *Annu Rev Microbiol* **57:** 579–608.

Schofield, M.J., Brownewell, F.E., Nayak, S., Du, C., Kool, E.T., and Hsieh, P. (2001a) The Phe-X-Glu DNA binding motif of MutS. The role of hydrogen bonding in mismatch recognition. *J Biol Chem* **276:** 45505–45508.

Schofield, M.J., Nayak, S., Scott, T.H., Du, C., and Hsieh, P. (2001b) Interaction of *Escherichia coli* MutS and MutL at a DNA mismatch. *J Biol Chem* **276:** 28291–28299.

Shell, S.S., Putnam, C.D., and Kolodner, R.D. (2007) The N

terminus of *Saccharomyces cerevisiae* Msh6 is an unstructured tether to PCNA. *Mol Cell* **26:** 565–578.
Simmons, L.A., and Kaguni, J.M. (2003) The DnaAcos allele of *Escherichia coli*: hyperactive initiation is caused by substitution of A184V and Y271H, resulting in defective ATP binding and aberrant DNA replication control. *Mol Microbiol* **47:** 755–765.
Simmons, L.A., Grossman, A.D., and Walker, G.C. (2007) Replication is required for the RecA localization response to DNA damage in *Bacillus subtilis*. *Proc Natl Acad Sci USA* **104:** 1360–1365.
Simmons, L.A., Davies, B.W., Grossman, A.D., and Walker, G.C. (2008) Beta clamp directs localization of mismatch repair in *Bacillus subtilis*. *Mol Cell* **29:** 291–301.
Simmons, L.A., Goranov, A.I., Kobayashi, H., Davies, B.W., Yuan, D.S., Grossman, A.D., and Walker, G.C. (2009) Comparison of responses to double-strand breaks between *Escherichia coli* and *Bacillus subtilis* reveals different requirements for SOS induction. *J Bacteriol* **191:** 1152–1161.
Smith, B.T., Grossman, A.D., and Walker, G.C. (2001) Visualization of mismatch repair in bacterial cells. *Mol Cell* **8:** 1197–1206.
Stukenberg, P.T., Studwell-Vaughn, P.S., and O'Donnell, M. (1991) Mechanism of the sliding clamp of DNA polymerase III holoenzyme. *J Biol Chem* **266:** 11328–11334.
Su, S.S., and Modrich, P. (1986) *Escherichia coli mutS*-encoded protein binds to mismatched DNA base pairs. *Proc Natl Acad Sci USA* **83:** 5057–5061.
Su'etsugu, M., and Errington, J. (2011) The replicase sliding clamp dynamically accumulates behind progressing replication forks in *Bacillus subtilis* cells. *Mol Cell* **41:** 720–732.
Sullivan, N.L., Marquis, K.A., and Rudner, D.Z. (2009) Recruitment of SMC by ParB-parS organizes the origin region and promotes efficient chromosome segregation. *Cell* **137:** 697–707.
Teleman, A.A., Graumann, P.L., Lin, D.C., Grossman, A.D., and Losick, R. (1998) Chromosome arrangement within a bacterium. *Curr Biol* **8:** 1102–1109.
Tessmer, I., Yang, Y., Zhai, J., Du, C., Hsieh, P., Hingorani, M.M., and Erie, D.A. (2008) Mechanism of MutS searching for DNA mismatches and signaling repair. *J Biol Chem* **283:** 36646–36654.
Turrientes, M.C., Baquero, M.R., Sanchez, M.B., Valdezate, S., Escudero, E., Berg, G., *et al*. (2010) Polymorphic mutation frequencies of clinical and environmental *Stenotrophomonas maltophilia* populations. *Appl Environ Microbiol* **76:** 1746–1758.
Umar, A., Buermeyer, A.B., Simon, J.A., Thomas, D.C., Clark, A.B., Liskay, R.M., and Kunkel, T.A. (1996) Requirement for PCNA in DNA mismatch repair at a step preceding DNA resynthesis. *Cell* **87:** 65–73.
Walsh, B.W., Lenhart, J.S., Schroeder, J.W., and Simmons, L.A. (2012) Far Western blotting as a rapid and efficient method for detecting interactions between DNA replication and DNA repair proteins. *Methods Mol Biol* **922:** 161–168.
Watson, M.E., Jr, Burns, J.L., and Smith, A.L. (2004) Hypermutable *Haemophilus influenzae* with mutations in *mutS* are found in cystic fibrosis sputum. *Microbiology* **150:** 2947–2958.
Webb, C.D., Teleman, A., Gordon, S., Straight, A., Belmont, A., Lin, D.C., *et al*. (1997) Bipolar localization of the replication origin regions of chromosomes in vegetative and sporulating cells of *B. subtilis*. *Cell* **88:** 667–674.
Zhai, J., and Hingorani, M.M. (2010) *Saccharomyces cerevisiae* Msh2–Msh6 DNA binding kinetics reveal a mechanism of targeting sites for DNA mismatch repair. *Proc Natl Acad Sci USA* **107:** 680–685.

Supporting information

Additional supporting information may be found in the online version of this article.